Mathematical Biosciences and Engineering

MBE, 20(12): 21451–21466.
DOI: 10.3934/mbe.2023949
Received: 22 August 2023
Revised: 17 November 2023
Accepted: 22 November 2023
Published: 04 December 2023

http://www.aimspress.com/journal/MBE

Research article

Biomechanical study of the effect of traction on elbow joint capsule contracture

Fang Wang[1,2,*,†], Jiaming Wang[1], Mingxin Li[3,†], Jun Hu[1], Kehua Song[1], Jianguo Zhang[1] and Yubo Fan[4,5]

[1] College of Mechanical Engineering, The Key Laboratory of Integrated Design and On-Line Monitoring of Light Industrial and Food Engineering Machinery and Equipment in Tianjin, Tianjin University of Science & Technology, Tianjin 300222, China
[2] Key Laboratory of Rehabilitation Aids Technology and System of the Ministry of Civil Afairs, National Research Center for Rehabilitation Technical Aids, Beijing 100176, China
[3] Department of Traumatic Orthopaedics, Tianjin Hospital, Tianjin 300299, China
[4] Key Laboratory for Biomechanics and Mechanobiology of Ministry of Education, School of Biological Sciences and Medical Engineering, Beihang University, Beijing 100083, China
[5] Beijing Advanced Innovation Centre for Biomedical Engineering, Beihang University, Beijing 100083, China

† The authors contributed equally to this work.

* **Correspondence:** Email: fwang@tust.edu.cn.

Abstract: Dynamic orthoses have a significant effect on the treatment of elbow capsular contracture. Because of the lack of quantitative research on traction forces, determining the appropriate traction force to help stretch soft tissues and maintain the joint's range of motion is a challenge in the rehabilitation process. We developed a human elbow finite element (FE) model incorporating the activity behavior of the muscles and considering different capsular contracture locations, including total, anterior and posterior capsular contractures, to analyze the internal biomechanical responses of different capsular contracture models during flexion (30 to 80 degrees). Traction loads of 10, 20, 30 and 40 N were applied to the ulna and radius at the maximum flexion angle (80 degrees) to explore the appropriate traction loads at week 4 after a joint capsule injury. We observed a significant increase in posterior capsule stress with anterior capsular contracture (ACC), and the maximum peak stress was 1.3 times higher than that in the healthy model. During the fourth week after elbow capsule injury, the

appropriate traction forces for total capsule contracture (TCC), ACC and posterior capsule contracture (PCC) were 20, 10 and 20 N, respectively; these forces maintained a stable biomechanical environment for the elbow joint and achieved a soft tissue pulling effect, thus increasing elbow mobility. The results can be used as a quantitative guide for the rehabilitation physicians to determine the traction load for a specific patient.

Keywords: elbow joint contracture; finite element analysis; computational elbow model; stress; tractive force

1. Introduction

As an essential joint, the function of the elbow joint is closely related to the body's activity and quality of life. A statistical study showed a significant prevalence of serious elbow injuries brought on by sports, falls and auto accidents [1]. Although there are more comprehensive treatments for elbow injuries, the complex biomechanical environment and anatomy of the elbow joint often lead to elbow stiffness after injury [2,3]. Sojbjerg [4] reported that the incidence of post-traumatic elbow stiffness was about 5%. In contrast, Dunham et al. [5] suggested that the rate was as high as 50%. The development of elbow stiffness can have more adverse effects on the patient's emotional state and daily work. Therefore, in order to provide targeted rehabilitation treatment, it is valuable to comprehend the mechanical characteristics and the soft tissue stress distribution around the elbow joint following stiffness.

The upper arm and forearm are connected by the elbow joint. It consists of the lower end of the humerus and the upper ends of the ulna and radius. The three joints (both the ulnar, brachioradial and superior radial-ulnar joints) are encased in the same joint capsule. The ligaments are closely related to the joint capsule [6,7]. After suffering a relatively minor injury, the structural and biochemical properties of the joint capsule are altered, resulting in thickening, reduced compliance and loss of mobility [7,8]. Capsule contracture contributes significantly to elbow stiffness, and the most basic pathological change is a fibrotic contracture of the joint capsule [9–12]. Morrey et al. [13] found that an elbow range of motion of 30° to 130° could accomplish 90% of the activities required for daily life. With the significant changes in modern life and work styles, the range of motion of the elbow necessary for modern life requires even larger amounts of motion [14,15]. Elbow stiffness is defined as the limitation of extension > 30° and flexion < 120° [5]. According to research, a 50% decrease in elbow range of motion can result in an 80% loss in upper extremity function [7,16]. Therefore, the aim of treatment is to restore the above range of motion.

For elbow stiffness due to capsular contracture, dynamic orthoses can be used as a measure to improve functional elbow motion and avoid reoperation [17]. Dynamic orthoses generate continuous traction on contracted tissues through specific mechanical structures. Plastic deformation of the soft tissue is achieved on the basis of the creep mechanism [18], increasing the range of motion of the joint [17,19]. However, the appropriate traction load for the elbow is unknown. Overstretching during treatment can cause soft tissue tears leading to greater soft tissue contractures [20]. Inadequate traction prevents the joint from being in maximum flexion and extension resulting in a contracture that can recur [17]. Therefore, it is necessary to determine the appropriate traction force. Current researchers use dynamic orthotics primarily on the basis of the principle that more force is needed to remodel the

tissue [20]. A traction force of around 2N is used as a recommended value for the treatment of finger contractures [21], and it is clear that for the elbow a greater traction load is needed. Gluck et al. [22] used 40 N as the interaction force between the elbow and the orthosis to assess the biomechanical strength of the orthosis. Quantitative studies on the mechanical behavior of the interaction between the dynamic orthosis and the elbow joint during treatment are scarce [20,23,24]. Therefore, it is of practical interest to study the mechanical behavior of the elbow with a dynamic orthosis through biomechanical methods to select the appropriate traction force for the treatment of elbow contractures.

Finite element modeling is an important tool in the study of human biomechanical investigations. It is especially widely used to study hip and knee joints [25,26]. In addition, the emergence of new models has greatly enriched the field of biomechanical research [27–32]. Recently, several researchers have analyzed the biomechanics of the elbow joint with FE models. For example, Kamei et al. [33] constructed a FE model of the adult elbow to assess the effect of ulnar collateral ligament dysfunction on the stress and stress distribution in the humeral capitellum. Zarifian et al. [34] simulated different implants for the treatment of distal humerus fractures to determine the optimal implant configuration. Akkurt et al. [35] evaluated commonly used internal fixation of humeral shaft fractures with an FE model to provide further guidance to therapists. However, few studies have investigated FE models of joint capsular contracture, especially for traction treatment of the elbow joint.

In this study, we evaluated the effect of capsular contracture on the elbow joint using the FE approach to obtain appropriate traction. In addition, the mechanical behavior of traction in the treatment of elbow joint stiffness caused by joint capsular contracture was quantitatively evaluated. An FE model of the human elbow joint containing active muscle forces was created to simulate elbow joint traction with a dynamic orthosis. The results of the study provided a reference for the appropriate mechanical properties of different traction forces regarding joint capsular contracture.

2. Materials and methods

2.1. Establishment of the finite element model

Computed tomography (CT) images (map tomography thickness, 1 mm; resolution, 256 × 256) were obtained for the elbow of a healthy 43-year-old male volunteer who signed a consent form. The CT images were imported into Mimics (Materialise Technologies, Leuven, Belgium) software, and the humerus, radius and ulna were extracted through a threshold segmentation method. Then, Geomagic software (Geomagic, Inc., NC, USA) was used to fill and smooth the bone models to obtain a high-quality 3D elbow joint bone model. Hypermesh (Altair Engineering Inc., USA) was used to create the soft tissue of the elbow joint in the appropriate anatomical position, as directed by an orthopedic surgeon. The process of mesh delineation, assignment of material properties, loading and application of boundary conditions were also completed in Hypermesh. Hexahedral mesh has the advantages of good deformation characteristics and high computational accuracy, and the number of elements and nodes required to achieve the same accuracy is much less than that of tetrahedral mesh [36]. Furthermore, hexahedral elements showed improved convergence. Therefore, an eight-node hexahedral finite element was used for meshing each part of the elbow joint. The complete finite element model is shown in Figure 1, including the ligaments (medial collateral ligament and lateral ulnar collateral ligament), bones, muscles and articular cartilage. A total of 32,725 nodes and 27,648 elements were included in the FE model. Table 1 shows that the material properties of each part of the

model were derived from the data of several previous studies. Bone was analyzed biomechanically by treating it as an isotropic elastic material [37,38], which made the simulation results more accurate and closer to the real situation. Similarly, we defined ligaments, joint capsules, contractured capsule and articular cartilage as hyperelastic materials, following existing research [39–41].

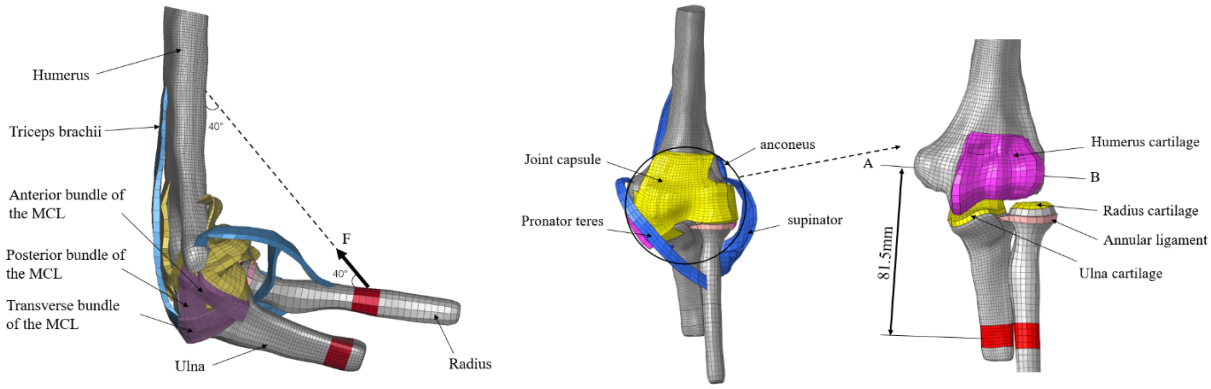

Figure 1. Elbow joint finite element model.

Table 1. QLV material constitutive model and Hill's muscle constitutive model.

Model parameters	Parameter values	Parameter description
ρ (g·mm^{-3})	1.06×10^{-3}	Density of the QLV model
v	0.495	Poisson's ratio of the QLV model
C_i	0.991; 0; 34.65	Instantaneous elastic response of the QLV model
G_i / MPa	0.697; 1.086; 0.102; 0.1	Viscous shear modulus of the QLV model
β_i / s^{-1}	589.1; 312.4; 1; 4.5×10^{-3}	Response to viscosity of the QLV model
$б_{Max}$ (MPa)	0.5	Maximum isometric contraction force
L_{opt}	1.05	Optimum length
Csh	0.45	Shape parameter of $f_{(x)}$
V_{Max} (m/s)	0.945	Maximum contraction velocity

Combining the passive nonlinear viscoelastic (QLV) element with the active Hill truss element allowed researchers to simulate both the active and passive dynamics of the muscle [42,43]. Integration of the nonlinear transient elastic response based on strain time produced the viscoelastic response of the QLV model. The instantaneous elastic response function, viscoelastic stress function, and viscoelastic stress relaxation function were defined by Eqs (1)–(3), respectively.

$$\sigma^e = \sum_i c_i \varepsilon^i, \tag{1}$$

$$\sigma = \int_0^t G(t-\tau)\frac{\partial \sigma^e}{\partial \varepsilon}\frac{\partial \varepsilon}{\partial \tau}d\tau, \tag{2}$$

$$G(t) = \sum_{z=1}^{n} G_i e^{-\beta_i t}. \tag{3}$$

where C_i and σ^e are the instantaneous elastic response parameters and instantaneous elastic response, σ and G_i are the total stress and relaxation modulus and β_i is the time constant. Equation (4) defined the active contraction force that the Hill model calculates.

$$F_{ce} = A(t)F_l(l)F_v(v)F_{max}. \tag{4}$$

where $F_v(v)$ and F_{max} are the muscle's velocity curve and maximal isometric contraction force, and A(t) and $F_l(l)$ are the muscle's activation level curve and length curve, respectively [43–45]. The parameters of the QLV material proprioceptive model and Hill muscle proprioceptive model are recorded in Table 1.

2.2. Model validation

Validation of the finite element model was completed by us. The validity of the model was demonstrated by applying forces ranging from 98 N to 490 N to the humeral interface, and the stress at the contact surface of the brachioradial joint was compared with the experimental findings of Takatori et al. [46]. The details of the validation procedure can be found in the literature [47].

2.3. Finite element model of elbow contracture

Stretching with a dynamic orthosis within two weeks of elbow capsule injury may be counterproductive. Stretching traction caused additional differentiation of myofibroblasts, leading to further contracture of the joint capsule [2]. Dynamic orthoses may be appropriate three to four weeks after an elbow injury. At this time, collagen fibers are gradually forming and the orientation of the collagen fibers is determined by the direction of mechanical tension [48]. We chose to simulate a traction load intervention during the fourth week after the joint capsule injury. Early myofibroblasts were distributed in the anterior or posterior part of the joint capsule or both. In addition, clinical studies have suggested that myofibroblasts are an important cause of joint capsule contracture [2]. Therefore, three types of joint capsule contracture were considered in this paper: Total capsule contracture, anterior capsule contracture and posterior capsule contracture. The joint capsule was divided by us into anterior and posterior capsules according to the anatomical structure. The material parameters of the contractured capsule in Table 2 were assigned to the anterior capsule, posterior capsule and total capsule to realize the anterior capsular contracture model (ACC), posterior capsular contracture model (PCC) and total capsular contracture model (TCC). The healthy model was also assigned material parameters according to Table 2.

Table 2. Material properties of members in finite element model of elbow joint.

Components	Elasticity's modulus (MPa)	Poisson's ratio
Bone	15,000	0.3
Articular cartilage	Neo-Hookean, C10 = 1.79	
Healthy capsule	Neo-Hookean, C10 = 1.44	
Ligaments	Neo-Hookean, C10 = 1.44	
Contractured capsule	Neo-Hookean, C10 = 1.66	

2.4. Boundary conditions and loading

In this model, the humerus was completely fixed, and the ulna and radius could be rotated only around the flexion axis. According to clinical statistics, the average restriction angle of the contractured elbow joint in flexion is 80 degrees [49]. Therefore, we used a flexion angle between 30 and 80 degrees. This work modeled elbow flexion under three conditions using an angular velocity of 1 rad/s [50,51]. TCC, ACC and PCC. Hackl et al. [52] fixed the elbow joint in flexion on a test stand. When the load was applied to the shaft end of the humerus, the forces through the ulnar-humeral and radial-humeral joints were approximately 25 and 75%, respectively. Therefore, at 80 degrees of elbow flexion, the traction forces were loaded on the ulna and radius at 25 and 75%, respectively, so that the FE model was closer to the actual force situation (Figure 1). The traction load sizes were 10, 20, 30 and 40 N. In addition, the distance between the position of the traction load application and the position of the axis of rotation of the elbow joint was approximately 81.5 mm, and the bending moments were approximately 0.524 N · m, 1.048 N · m, 1.572 N · m and 2.065 N · m [52].

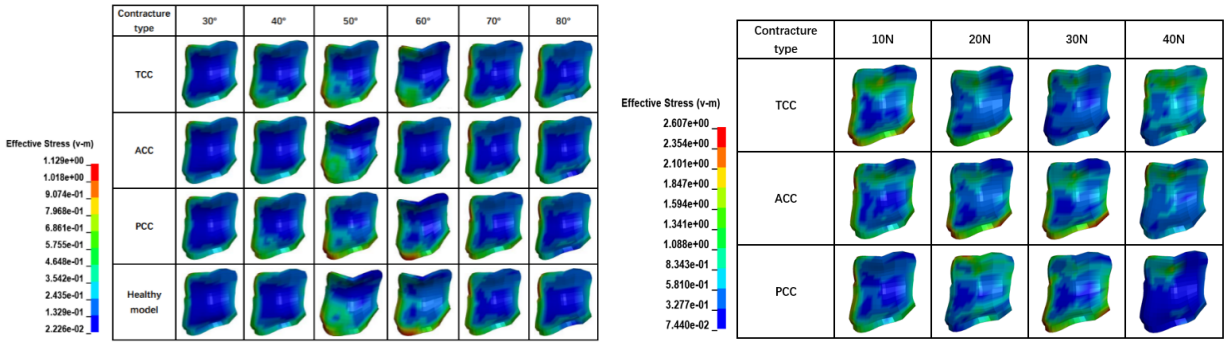

(a) (b)

Figure 2. (a) Stress transmission on the ulnar cartilage contact surfaces of the healthy model, TCC, ACC and PCC when the elbow joint was flexed at 30–80 degrees with an angular velocity of 1 rad/s; (b) Comparison of ulnar cartilage stress distribution in TCC, ACC and PCC under conditions of traction with different loads when the elbow joint was at a maximum flexion angle of 80 degrees.

3. Results

3.1. Stress situation in soft tissues

Figure 2(a) shows how the ulnar cartilage (UC) was stressed during elbow flexion. The distribution of ulnar cartilage stress was very similar in TCC and PCC. In the initial phase of flexion, the ulnar cartilage stress was small, and the change was not apparent. As the flexion angle increased, the stress moved to the anterior medial side and reached its peak on the anterior medial side. At the end of flexion, the ulnar cartilage stress shifted toward the posterior medial side. Figure 2(b) demonstrates the ulnar cartilage stress distribution for the three contracture models under the four traction loads and shows significant changes in ulnar cartilage stress for each model after applying the traction loads. The stresses on the ulnar cartilage under traction were distributed on the edge and posterior medial side of the ulnar cartilage. During TCC, the ulnar cartilage stress distribution at 20 N

was similar to that of the ulnar cartilage at 30 N, and during ACC, the ulnar cartilage stress distribution at 10 N was similar to that of the ulnar cartilage at 40 N. Figure 3 presents the changing traits of stress in the ligaments and cartilage under different stimuli. Compared with the healthy model, we observed a marked increase in stresses in all soft tissues except the anterior capsule and the transverse bundle of the MCL (tMCL) under different traction load conditions.

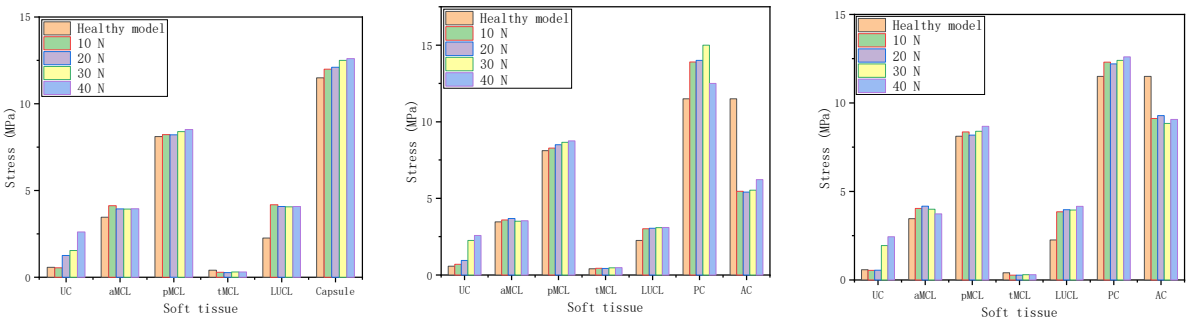

(a) TCC (b) ACC (c) PCC

Figure 3. (a) Soft tissue stresses under different traction loads during TCC; (b) Soft tissue stresses under different traction loads during ACC; and (c) Soft tissue stresses under different traction loads during PCC.

Stress trends in ulnar cartilage were similar for TCC and PCC (Figure 4(a)), with elevated ulnar cartilage stress between 30 and 50 degrees, and both were greater than ulnar cartilage stress in healthy model flexion. From 50 degrees to 60 degrees, the ulnar cartilage stress decreased and was less than the ulnar cartilage stress in healthy model flexion between 60 and 70 degrees. The peak stress of PCC at a flexion angle of 70 degrees was 1.06 MPa, which was around 1.05 times the maximum stress of healthy model flexion. The trend of the change in stress in ACC between 30 and 50 degrees of flexion was the opposite of that in the other cases, with the highest stress of 1.167 MPa observed at 70 degrees of flexion. The stress values of the anterior bundle of the MCL (aMCL) and the posterior bundle of the MCL (pMCL) increased with an increasing flexion angle, as shown in Figure 4(b),(c). For the aMCL, the stress trends were essentially the same for TCC and PCC from 30 degrees to 60 degrees. Overall, we observed the highest stress values in the TCC and PCC had from 30 degrees to 80 degrees of flexion and the lowest stress values in healthy model flexion. The maximum peak stress at 80 degrees of flexion was 4.06 MPa (PCC), which was around 1.05 times the maximum flexion stress in the healthy model. The stress values of the pMCL in different states were very similar, and the stress values of TCC from 40 degrees to 60 degrees were the smallest. For the tMCL, the stress values for ACC and healthy model flexion were essentially the same, and the stress values for TCC from 30 degrees to 50 degrees were higher than those in the other cases. The TCC and PCC stress values from 50 degrees to 80 degrees were lower than those in the other two cases. The stress values for TCC and PCC from 50 degrees to 80 degrees were lower than those in the other two cases, and the peak stress for PCC decreased by 34% from that in healthy model flexion (Figure 4(d)). The difference in stress variation in the lateral ulnar collateral ligament (LUCL) was more pronounced, with a maximum peak stress in TCC and PCC 1.78 times greater than that in healthy model flexion (Figure 4(e)). The stress values of the anterior capsule in different states are shown in Figure 4(f). The ACC had the lowest stress value, with a 49% reduction in maximum peak stress from that in healthy model flexion. The TCC had the

largest stress value, with a maximum peak stress approximately 1.1 times higher than that in healthy model flexion. For the posterior capsule (Figure 4(g)), the ACC had the largest value of stress in the overall range of flexion, with a maximum peak stress approximately 1.3 times higher than that in the healthy model flexion stress value.

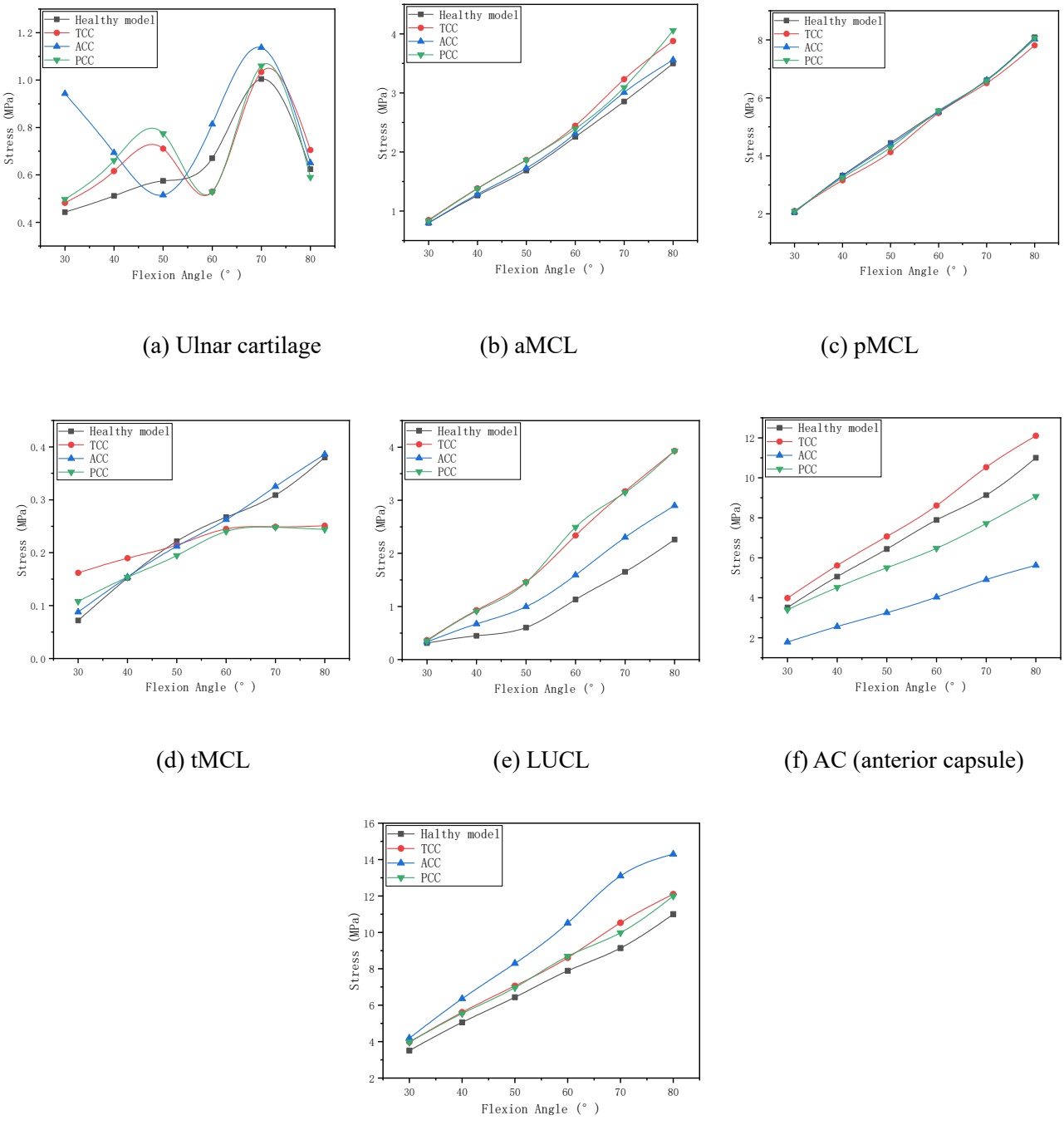

(a) Ulnar cartilage (b) aMCL (c) pMCL

(d) tMCL (e) LUCL (f) AC (anterior capsule)

(g) PC (posterior capsule)

Figure 4. Stress changes in (a) ulnar collateral cartilage, (b) aMCL, (c) pMCL, (d) tMCL, (e) LUCL, (f) AC and (g) PC when the elbow joint is flexed at an angular velocity of 1 rad/s for 30–80 degrees under healthy model, TCC, ACC and PCC conditions.

Table 3. Soft tissue stresses under different traction loads during TCC.

soft tissue	Healthy model (MPa)	10 N (MPa)	20 N (MPa)	30 N (MPa)	40 N (MPa)
UC	0.573	0.543	1.26	1.54	2.61
aMCL	3.46	4.13	3.94	3.93	3.95
pMCL	8.11	8.22	8.21	8.4	8.52
tMCL	0.405	0.285	0.27	0.306	0.305
LUCL	2.26	4.18	4.08	4.06	4.08
Capsule	11.5	12	12.1	12.5	12.6

Table 4. Soft tissue stresses under different traction loads during ACC.

soft tissue	Healthy model (MPa)	10 N (MPa)	20 N (MPa)	30 N (MPa)	40 N (MPa)
UC	0.573	0.691	0.951	2.26	2.58
aMCL	3.46	3.59	3.68	3.51	3.54
pMCL	8.11	8.28	8.5	8.65	8.75
tMCL	0.405	0.429	0.421	0.471	0.474
LUCL	2.26	3.02	3.05	3.09	3.1
PC	11.5	13.9	14	15	12.5
AC	11.5	5.46	5.41	5.53	6.22

Table 5. Soft tissue stresses under different traction loads during PCC.

soft tissue	Healthy model (MPa)	10 N (MPa)	20 N (MPa)	30 N (MPa)	40 N (MPa)
UC	0.573	0.533	0.55	1.94	2.44
aMCL	3.46	4.04	4.17	3.99	3.73
pMCL	8.11	8.36	8.18	8.4	8.68
tMCL	0.405	0.267	0.27	0.293	0.296
LUCL	2.26	3.85	3.97	3.95	4.15
PC	11.5	12.3	12.2	12.4	12.6
AC	11.5	9.12	9.28	8.84	9.06

4. Discussion

Dynamic orthoses are an effective means of treating elbow stiffness and restoring the functional arc of motion to the elbow [2]. The treatment process requires appropriate traction to achieve soft tissue plastic deformation and thus increase elbow mobility. Currently, improvement in elbow mobility in rehabilitation is mainly observed with macroscopic movements [19,24]. The internal biomechanics of the elbow joint is complex, and the study of stress in the soft tissue of the elbow under the state of capsular contracture is not completely clear. Furthermore, quantitative studies on the mechanical behavior of the interaction between the dynamic orthosis and the elbow joint are scarce. In this study, we developed a healthy model, TCC model, ACC model and PCC model. First, we assessed the stresses of different types of soft tissues in the elbow joint during flexion in comparison with the healthy model to provide constructive options for traction force treatment for elbow joint contracture. Then, we investigated the mechanical response of the elbow joint after applying the traction load to determine the appropriate traction load.

The results showed that the soft tissue stress values were very similar for TCC and PCC, and the ulnar cartilage stress distribution was also very similar. In the range of 50 to 60 degrees of flexion, the stress on the posterior medial aspect of the ulnar cartilage was transferred to the anterior medial aspect of the ulnar cartilage, where the notch of the ulnar trochlear was located. This was consistent with clinical autopsy results [53]. In addition, the distribution and transfer of ulnar cartilage stress in TCC and PCC during elbow flexion were comparable to those in healthy model flexion (Figure 2(a)). In the range of 30 degrees to 50 degrees, ulnar stresses in TCC and PCC were greater than those in the healthy model and increased with an increasing flexion angle (Figure 4(a)). The ulnar cartilage stress was reduced by 18% (at 50 degrees) in TCC compared with PCC. This suggests that ulnar cartilage stress was less affected by the anterior capsule. Therefore, we hypothesized that the posterior capsule plays a greater role in the flexion process than the anterior capsule after the contracture of the joint capsule. This was consistent with the findings of King et al. [54]. When the elbow was flexed from 30 to 80 degrees, more posterior capsule stress was observed in the ACC state than in other situations (Figure 4(g)). According to reports, the collagen fibers in the healthy anterior capsule were extremely dispersed and relatively thin and elastic [11]. We speculated that the reduced flexibility of the contracted anterior capsule created an obstacle in the process of elbow flexion, resulting in increased stress on the posterior capsule. This finding was consistent with the findings of Gallay et al. [55], who found that the compliance of the contracted elbow capsule was one-sixth that of the healthy elbow joint. We further hypothesized that for the ACC condition, traction should not be excessive to avoid straining the posterior capsule. We found that posterior capsular contracture and total capsular contracture had a greater effect on tMCL stress during 60 to 80 degrees of elbow flexion, whereas anterior capsular contracture had little effect on tMCL stress (Figure 4(d)). This suggests that there is some connection between the posterior capsule and the tMCL. The reason for this we can find an explanation in the anatomic structure of the elbow. Kimata et al. [56] found that the tMCL is strongly connected to the posterior capsule. tMCL contributes the least to the stability of the contracted elbow joint [57]. When the posterior capsule is contracted, the stress on the tMCL decreases and its contribution to elbow stability is further weakened. This was an additional finding of this study.

Higher traction forces can lead not only to soft tissue injuries but also to the instability of the elbow joint. Morrey et al. [58] reported that the articular surface of the superior ulna was the primary stabilizer of the elbow joint. Joint instability is indicated by changes in the ulnar cartilage stress distribution compared with a healthy model. Therefore, it was necessary to analyze the stability of the elbow joint by comparing the stress distribution of the ulnar cartilage under various traction forces. We compared the ulnar cartilage stress distribution in a contracture model loaded with traction (Figure 2(b)) and in a healthy model flexed to 80 degrees (Figure 2(a)). The stress distribution of the ulnar cartilage under 20 and 30 N traction loads during TCC (Figure 2(b)) was similar to that of the ulnar cartilage of the healthy model with a flexion angle of 80 degrees (Figure 2(a)). This phenomenon showed that the elbow joint with TCC was more stabilized by traction loads of 20 and 30 N than by traction loads of 10 and 40 N. By analyzing Table 3 and Figure 3(a), we found that in TCC, the stress values of each soft tissue at 20 N were closer to those in the healthy model than at 30 N. It was reported that low load traction helped the tissue slowly undergo plastic deformation [19]. Consequently, it was important to focus on the traction load that brought the stress values of each soft tissue of the contractured elbow joint close to the stress values of each soft tissue in the healthy model while maintaining the stability of the elbow joint. This showed that the elbow joint with TCC was more conducive to tissues slowly undergoing plastic deformation by traction loads of 20 N than by traction

loads of 30 N. Thus, the appropriate traction force for the elbow joint with TCC was determined to be 20 N. Following the same approach, we found that the stress distribution of the ulnar cartilage under 10 N and 40 N traction loads during ACC (Figure 2(b)) was similar to that of the ulnar cartilage of the healthy model with a flexion angle of 80 degrees (Figure 2(a)). As stated in the previous paragraph, we concluded that the traction load should not be excessive in ACC. As shown in Table 4 and Figure 3(b), we found that in ACC, the stress values of each soft tissue at 10 N were more similar to those in the healthy model than at 40 N. Consequently, the appropriate traction force for the elbow joint with ACC was determined to be 10 N. The stress distribution of the ulnar cartilage under 10 and 20 N traction loads during PCC (Figure 2(b)) was similar to that of the ulnar cartilage of the healthy model with a flexion angle of 80 degrees (Figure 2(a)). As shown in Table 5 and Figure 3(c), we found that in PCC, the stress values of each soft tissue at 20 N were more similar to those in the healthy model than at 10 N. Therefore, we determined that the appropriate traction force for the elbow joint with PCC was 20 N. The results showed that most of the soft tissue stress values increased under all four traction loads, indicating that the traction loads exerted pull on the soft tissues, which is consistent with the creep mechanism of the dynamic orthosis in the actual treatment process [19]. Unsuitable traction can lead to soft tissue tears [20], which can be painful. We also found that unsuitable traction can lead to changes in the stress distribution in the ulnar cartilage, which may be responsible for the patient's discomfort.

Although many studies have investigated the treatment of elbow contractures with braces, few studies have assessed the selection of appropriate traction for the treatment of elbow contractures. At this stage, researchers have mainly applied traction forces based on the principle that more force is needed to remodel the tissue [20]. In addition, many studies have been conducted to evaluate the clinical efficacy of dynamic orthoses for the treatment of elbow contractures [59–61] and focused on the mechanical design of dynamic orthoses [62–65]. The traction in our study can be used as a reference for clinical treatment to achieve satisfactory therapeutic results. The method can also be combined with a clinical approach to customize rehabilitation programs for specific patients based on the different contracture locations of the elbow joint.

This study was limited by the simplification of the FE model. Because of this, the model could not respond to the elbow biomechanical environment with high accuracy. In addition, the model developed in this work simulated the state of traction load intervention during the fourth week of joint capsule injury. However, traction bracing for elbow stiffness is a long-term process [23]. In this study, we did not account for the long-term behavior of the traction support with the elbow. As the soft tissues of the elbow undergo plastic deformation by traction, the material properties and internal structure of the soft tissues are altered [19]. Therefore, in a future study, we will consider this biological process by studying soft tissue material properties in animal models.

5. Conclusions

We constructed a finite element model of the elbow to simulate the flexion process of the contracted elbow and investigated the mechanical response of the elbow joint after applying the traction load. We observed a significant increase in posterior capsule stress with anterior capsular contracture, and the maximum peak stress was 1.3 times higher than that in the healthy model. The traction load was shown to have a significant effect on the biomechanical response of the elbow joint. The appropriate traction forces for total, anterior and posterior capsular contractures were 20, 10 and 20

N, respectively, in the fourth week after elbow capsule injury, which could maintain a stable biomechanical environment for the elbow joint and achieve a soft tissue pulling effect, thereby increasing elbow mobility. The results could provide quantitative guidance to the rehabilitation physician in determining the traction load for a specific patient.

Use of AI tools declaration

The authors declare they have not used Artificial Intelligence (AI) tools in the creation of this article.

Acknowledgments

This study was supported by funds from National Natural Science Foundation of China (NSFC) Research Grants (12102301; 31871212; 51975411).

Conflict of interest

The authors declare that there are no conflicts of interest.

References

1. J. W. Stoneback, B. D. Owens, J. Sykes, G. S. Athwal, L. Pointer, J. M. Wolf, Incidence of elbow dislocations in the United States population, *J. Bone Jt. Surg.*, **94** (2012), 240–245. https://doi.org/10.2106/JBJS.J.01663
2. J. N. Doornberg, T. Bosse, M. S. Cohen, J. B. Jupiter, D. Ring, P. Kloen, Temporary presence of myofibroblasts in human elbow capsule after trauma, *J. Bone Jt. Surg.*, **96** (2014), e36. https://doi.org/10.2106/JBJS.M.00388
3. A. L. C. Lindenhovius, J. B. Jupiter, The posttraumatic stiff elbow: A Review of the Literature, *J. Hand Surg.*, **32** (2007), 1605–1623. https://doi.org/10.1016/j.jhsa.2007.09.015.
4. J. O. Sajbjerg, The stiff elbow: How I do it, *Acta Orthop. Scand.*, **67** (1996), 626–631. https://doi.org/10.3109/17453679608997771
5. C. L. Dunham, R. M. Castile, N. Havlioglu, A. M. Chamberlain, S. P. Lake, Temporal patterns of motion in flexion-extension and pronation-supination in a rat model of posttraumatic elbow contracture, *Clin. Orthop. Relat. Res.*, **476** (2018), 1878–1889. https://doi.org/10.1097/CORR.0000000000000388
6. L. E. Karbach, J. Elfar, Elbow Instability: Anatomy, biomechanics, diagnostic maneuvers, and testing, *J. Hand Surg.*, **42** (2017), 118–126. https://doi.org/10.1016/j.jhsa.2016.11.025
7. B. Attum, W. Obremskey, Posttraumatic elbow stiffness: A critical analysis review, *JBJS Rev.*, **4** (2016). https://doi.org/10.2106/JBJS.RVW.15.00084
8. D. Ring, J. B. Jupiter, Operative treatment of elbow stiffness, *JBJS Essent. Surg. Tech.*, **1** (2011), e18. https://doi.org/10.2106/jbjs.st.k.00010
9. K. A. Hildebrand, M. Zhang, A. D. Befus, P. T. Salo, D. A. Hart, A myofibroblast-mast cell-neuropeptide axis of fibrosis in post-traumatic joint contractures: An in vitro analysis of mechanistic components, *J. Orthop. Res.*, **32** (2014), 1290–1296. https://doi.org/10.1002/jor.22676

10. J. N. Doornberg, T. Bosse, M. S. Cohen, J. B. Jupiter, D. Ring, P. Kloen, Temporary presence of myofibroblasts in human elbow capsule after trauma, *J. Bone Jt. Surg.*, **96** (2014), e36. https://doi.org/10.2106/JBJS.M.00388
11. M. S. Cohen, D. R. Schimmel, K. Masuda, H. Hastings, C. Muehleman, Structural and biochemical evaluation of the elbow capsule after trauma, *J. Shoulder Elbow Surg.*, **16** (2007), 484–490. https://doi.org/10.1016/j.jse.2006.06.018
12. L. M. Reichel, O. A. Morales, Gross anatomy of the elbow capsule: A cadaveric study, *J. Hand Surg.*, **38** (2013), 110–116. https://doi.org/10.1016/j.jhsa.2012.09.031
13. B. F. Morrey, L. J. Askew, E. Y. Chao, A biomechanical study of normal functional elbow motion, *J. Bone Jt. Surg.*, **63** (1981), 872–877. https://doi.org/10.2106/00004623-198163060-00002
14. G. Bhabra, C. S. Modi, T. Lawrence, Managing the stiff elbow, *Orthop. Trauma*, **30** (2016), 329–335. https://doi.org/10.1016/j.mporth.2016.04.005
15. C. C. L. Yau, J. Viveen, D. Eygendaal, B. The, Management of the stiff elbow, *Orthop. Trauma*, **34** (2020), 206–212. https://doi.org/10.1016/j.mporth.2020.05.003
16. R. Sivakumar, V. Somasheker, P. K. Shingi, T. Vinoth, M. Chidambaram, Treatment of stiff elbow in young patients with interpositional arthroplasty for mobility: Case Series, *J. Orthop. Case Rep.*, **6** (2016), 49–52. https://doi.org/10.13107/jocr.2250-0685.566
17. A. M. G. Cavalcanti, R. S. O. Filho, H. C. Gomes, A. B. S. Martins, E. B. Garcia, L. M. Ferreira, Review of articulated elbow orthotics for joint stiffness rehabilitation, *Acta Ortop. Bras.*, **30** (2022), e254358. https://doi.org/10.1590/1413-785220223005e254358
18. P. M. Bonutti, J. E. Windau, B. A. Ables, B. G. Miller, Static progressive stretch to reestablish elbow range of motion, *Clin. Orthop. Relat.*, **303** (1994), 128–134. https://doi.org/10.1097/00003086-199406000-00015
19. G. L. Gallucci, J. G. Boretto, M. A. Dávalos, A. Donndorff, V. A. Alfie, P. De Carli, Dynamic splint for the treatment of stiff elbow, *Shoulder Elbow*, **3** (2011), 52–55. https://doi.org/10.1111/j.1758-5740.2010.00096.x
20. G. Sim, J. Fleming, C. Glasgow, Mobilizing orthoses in the management of post-traumatic elbow contractures: A survey of Australian hand therapy practice, *J. Hand Ther.*, **34** (2021), 90–99. https://doi.org/10.1016/j.jht.2019.12.014
21. N. Young, N. Terrington, D. Francis, L. S. Robinson, Orthotic management of fixed flexion deformity of the proximal interphalangeal joint following traumatic injury: A systematic review, *Hong Kong J. Occup. Ther.*, **31** (2018), 3–13. https://doi.org/10.1177/1569186118764067
22. M. J. Gluck, C. M. Beck, K. M. Sochol, D. A. London, M. R. Hausman, Comparative strength of elbow splint designs: a new splint design as a stronger alternative to posterior splints, *J. Shoulder Elbow Surg.*, **28** (2019), e125–e130. https://doi.org/10.1016/j.jse.2018.10.015
23. A. L. C. Lindenhovius, J. N. Doornberg, K. M. Brouwer, J. B. Jupiter, C. S. Mudgal, D. Ring, A prospective randomized controlled trial of dynamic versus static progressive elbow splinting for posttraumatic elbow stiffness, *J. Bone Jt. Surg.*, **94** (2012), 694–700. https://doi.org/10.2106/JBJS.J.01761
24. G. L. Gallucci, J. G. Boretto, M. A. Dávalos, A. Donndorff, V. A. Alfie, P. D. Carli, Dynamic splint for the treatment of stiff elbow, *Shoulder Elbow*, **3** (2011), 52–55. https://doi.org/10.1111/j.1758-5740.2010.00096.x

25. M. Li, M. S. Venäläinen, S. S. Chandra, R. Patel, J. Fripp, C. Engstrom, et al., Discrete element and finite element methods provide similar estimations for hip joint contact mechanics during walking gait, *J. Biomech.*, **115** (2021), 110163. https://doi.org/10.1016/j.jbiomech.2020.110163
26. M. E. Mononen, J. S. Jurvelin, R. K. Korhonen, Effects of radial tears and partial meniscectomy of lateral meniscus on the knee joint mechanics during the stance phase of the gait cycle-A 3D finite element study, *J. Orthop. Res.*, **31** (2013), 1208–1217. https://doi.org/10.1002/jor.22358
27. P. Xiang, K. M. Liew, Predicting buckling behavior of microtubules based on an atomistic-continuum model, *Int. J. Solids Struct.*, **48** (2011), 1730–1737. https://doi.org/10.1016/j.ijsolstr.2011.02.022
28. P. Xiang, K. M. Liew, Dynamic behaviors of long and curved microtubules based on an atomistic-continuum model, *Comput. Methods Appl. Mech. Eng.*, (2012), 123–132. https://doi.org/10.1016/j.cma.2012.02.023
29. P. Xiang, K. M. Liew, Free vibration analysis of microtubules based on an atomistic-continuum model, *J. Sound Vib.*, **331** (2012), 213–230. https://doi.org/10.1016/j.jsv.2011.08.024
30. P. Xiang, K. M. Liew, A computational framework for transverse compression of microtubules based on a higher-order Cauchy-Born rule, *Comput. Methods Appl. Mech. Eng.*, **254** (2013), 14–30. https://doi.org/10.1016/j.cma.2012.10.013
31. P. Xiang, L. W. Zhang, K. M. Liew, Analysis of macromolecular microtubules using the potential-based matrix displacement method, *Compos. Struct.*, **127** (2015), 224–230. https://doi.org/10.1016/j.compstruct.2015.03.004
32. P. Xiang, L. W. Zhang, K. M. Liew, A mesh-free computational framework for predicting vibration behaviors of microtubules in an elastic medium, *Compos. Struct.*, **149** (2016), 41–53. https://doi.org/10.1016/j.compstruct.2016.03.063
33. K. Kamei, E. Sasaki, K. Fujisaki, Y. Harada, Y. Yamamoto, Y. Ishibashi, Ulnar collateral ligament dysfunction increases stress on the humeral capitellum: a finite element analysis, *JSES Int.*, **5** (2021), 307–313. https://doi.org/10.1016/j.jseint.2020.10.022
34. A. Zarifian, A. A. Fough, D. Eygendaal, M. Rivlin, S. A. M. Shaegh, A. R. Kachooei, Length of plates and number of screws for the fixation of distal humerus fractures: A finite element biomechanical study, *J. Hand Surg.*, **47** (2022), 690. https://doi.org/10.1016/j.jhsa.2021.07.010
35. E. Akkurt, M. Yıldırım, F. Erenler, O. M. Tosun, M. F. Akkurt, B. Akkurt, et al., Mechanical evaluation for the finite element analysis of intramedullary nailing and plate screw system used in humerus transverse fractures, *J. Orthop*., 2023. https://doi.org/10.1016/j.jor.2023.10.024
36. A. Schonning, B. Oommen, I. Ionescu, T. Conway, Hexahedral mesh development of free-formed geometry: The human femur exemplified, *Comput. Aided Design*, **41** (2009), 566–572. https://doi.org/10.1016/j.cad.2007.10.007
37. M. Bendjaballah, A. Shirazi-Adl, D. Zukor, Finite element analysis of human knee joint in varus-valgus, *Clin. Biomech.*, **12** (1997), 139–148. https://doi.org/10.1016/S0268-0033(97)00072-7
38. J. G. Zhang, F. Wang, R. Zhou, Q. Xue, A three-dimensional finite element model of the cervical spine: an investigation of whiplash injury, *Med. Biol. Eng. Comput.*, **49** (2011), 193–201. https://doi.org/10.1007/s11517-010-0708-9
39. P. Büchler, N. A. Ramaniraka, L. R. Rakotomanana, J. P. Iannotti, A. Farron, A finite element model of the shoulder: application to the comparison of normal and osteoarthritic joints, *Clin. Biomech.*, **17** (2002), 630–639. https://doi.org/10.1016/S0268-0033(02)00106-7

40. K. M. Quapp, J. A. Weiss, Material characterization of human medial collateral ligament, *J. Biomech. Eng.*, **120** (1998), 757–763. https://doi.org/10.1115/1.2834890
41. M. M. Schulz, T. Q. Lee, M. D. Sandusky, J. E. Tibone, P. J. McMahon, The healing effects on the biomechanical properties of joint capsular tissue treated with Ho:YAG laser: An in vivo rabbit study, *Arthroscopy*, **17** (2001), 342–347. https://doi.org/10.1053/jars.2001.19677
42. F. Li, H. Li, W. Hu, S. Su, B. Wang, Simulation of muscle activation with coupled nonlinear FE models, *J. Mech. Med. Biol.*, **16** (2016), 1650082. https://doi.org/10.1142/S0219519416500822
43. S. Hedenstierna, P. Halldin, K. Brolin, Evaluation of a combination of continuum and truss finite elements in a model of passive and active muscle tissue, *Comput. Methods Biomech. Biomed. Eng.*, **11** (2008), 627–639. https://doi.org/10.1080/17474230802312516
44. B. S. Myers, C. A. V. Ee, D. L. A. Camacho, C. T. Woolley, T. M. Best, On the structural and material properties of mammalian skeletal muscle and its relevance to human, *Cervical Impact Dyn.*, **104** (1995), 3095–3105. https://doi.org/10.4271/952723
45. B. S. Myers, C. T. Woolley, T. L. Slotter, W. E. Garrett, T. M. Best, The influence of strain rate on the passive and stimulated engineering stress-large strain behavior of the rabbit tibialis anterior muscle, *J. Biomech. Eng.*, **120** (1998), 126–132. https://doi.org/10.1115/1.2834292
46. K. Takatori, H. Hashizume, H. Wake, H. Inoue, N. Nagayama, Analysis of stress distribution in the humeroradial joint, *J. Orthop. Sci.*, **7** (2002), 650–657. https://doi.org/10.1007/s007760200116
47. F. Wang, S. Jia, M. Li, K. Pan, J. Zhang, Y. Fan, Effect of the medial collateral ligament and the lateral ulnar collateral ligament injury on elbow stability: a finite element analysis, *Comput. Methods Biomech. Biomed. Eng.*, **24** (2021), 1517–1529. https://doi.org/10.1080/10255842.2021.1898601
48. L. Verstuyft, P. Caekebeke, R. van Riet, Postoperative rehabilitation in elbow surgery, *J. Clin. Orthop. Trauma.*, **20** (2021), 101497. https://doi.org/10.1016/j.jcot.2021.101479
49. Z. Y. Sun, *Development of a New Classification and Functional Score for Elbow Stiffness and Exploration of Long-Term Clinical Outcomes of Open Arthrolysis*, Ph.D thesis, Shanghai Jiao Tong University, 2020. https://doi.org/10.27307/d.cnki.gsjtu.2020.000096
50. T. K. K. Koo, A. F. T. Mak, A neuromusculoskeletal model to simulate the constant angular velocity elbow extension test of spasticity, *Med. Eng. Phys.*, **28** (2006), 60–69. https://doi.org/10.1016/j.medengphy.2005.03.012
51. T. Kodek, M. Munih, An analysis of static and dynamic joint torques in elbow flexion-extension movements, *Simul. Modell. Pract. Theory*, **11** (2003), 297–311. https://doi.org/10.1016/S1569-190X(03)00063-7
52. M. Hackl, K. Wegmann, S. L. Kahmann, N. Heinze, M. Staat, L. P. Müller, et al., Radial shortening osteotomy reduces radiocapitellar contact pressures while preserving valgus stability of the elbow, *Knee Surg. Sport Traumatol. Arthroscopy*, **25** (2017), 2280–2288. https://doi.org/10.1007/s00167-017-4468-z
53. K. Takatori, H. Hashizume, H. Wake, H. Inoue, N. Nagayama, Analysis of stress distribution in the humeroradial joint, *J. Orthop. Sci.*, **7** (2002), 650–657. https://doi.org/10.1007/s007760200116
54. G. J. W. King, B. F. Morrey, K. N. An, Stabilizers of the elbow, *J. Shoulder Elbow Surg.*, **2** (1993), 165–174. https://doi.org/10.1016/S1058-2746(09)80053-0

55. S. H. Gallay, R. R. Richards, S. W. O'Driscoll, Intraarticular capacity and compliance of stiff and normal elbows, *Arthroscopy*, **9** (1993), 9–13. https://doi.org/10.1016/S0749-8063(05)80336-6
56. K. Kimata, M. Yasui, H. Yokota, S. Hirai, M. Naito, T. Nakano, Transverse ligament of the elbow joint: an anatomic study of cadavers, *J. Shoulder Elbow Surg.*, **28** (2019), 2253–2258. https://doi.org/10.1016/j.jse.2019.04.048
57. G. F. Solitro, R. Fattori, K. Smidt, C. Nguyen, M. M. Morandi, R. S. Barton, Role of the transverse ligament of the ulnar collateral ligament of the elbow: a biomechanical study, *JSES Int.*, **5** (2021), 549–553. https://doi.org/10.1016/j.jseint.2021.01.009
58. B. F. Morrey, K. N. An, Stability of the elbow: Osseous constraints, *J. Shoulder Elbow Surg.*, **14** (2005), S174–S178. https://doi.org/10.1016/j.jse.2004.09.031
59. C. L. B. Guglielmetti, M. E. C. Gracitelli, J. H. Assunção, F. B. Andrade-Silva, M. M. N. Pessa, A. A. Ferreira-Neto, et al., Randomized trial for the treatment of post-traumatic elbow stiffness: surgical release vs. rehabilitation, *J. Shoulder Elbow Surg.*, **29** (2020), 1522–1529. https://doi.org/10.1016/j.jse.2020.03.023
60. E. S. Veltman, J. N. Doornberg, D. Eygendaal, M. P. J. van den Bekerom, Static progressive versus dynamic splinting for posttraumatic elbow stiffness: a systematic review of 232 patients, *Arch. Orthop. Trauma. Surg.*, **135** (2015), 613–617. https://doi.org/10.1007/s00402-015-2199-5
61. C. C. L. Yau, J. Viveen, D. Eygendaal, B. The, Management of the stiff elbow, *Orthop. Trauma.*, **34** (2020), 206–212. https://doi.org/10.1016/j.mporth.2020.05.003
62. E. Mobedi, W. Kim, M. Leonori, N. G. Tsagarakis, A. Ajoudani, Design and control of an assistive device for elbow effort-compensation, *IEEE/ASME Trans. Mechatron.*, 2023. https://doi.org/10.1109/TMECH.2023.3267681
63. M. Ceccarelli, M. Riabtsev, A. Fort, M. Russo, M. A. Laribi, M. Urizar, Design and experimental characterization of l-CADEL v2, an assistive device for elbow motion, *Sensors*, **21** (2021), 1–15. https://doi.org/10.3390/s21155149
64. J. D. A. Rosero, D. C. B. Rosero, L. F. A. Realpe, A. F. S. Pino, E. R. González, Mechatronic Design of a prototype orthosis to support elbow joint rehabilitation, *Bioengineering*, **9** (2022), 287. https://doi.org/10.3390/bioengineering9070287
65. R. Guachi, F. Napoleoni, F. Pipitone, M. Controzzi, Preliminary design and development of a selectable stiffness joint for elbow orthosis, in *2022 IEEE-RAS 21st International Conference on Humanoid Robots (Humanoids)*, (2022), 458–463. https://doi.org/10.1109/Humanoids53995.2022.10000188

AIMS Press